

# Extended Gravity Constraints at Different Scales

Stanislav Alexeyev<sup>1,2</sup>, Vyacheslav Prokopov<sup>1,3</sup>

<sup>1</sup> Sternberg Astronomical Institute, Lomonosov Moscow State University, Universitetskii Prospekt, 13, Moscow 119234, Russia;

<sup>2</sup> Department of Quantum Theory and High Energy Physics, Physics Faculty, Lomonosov Moscow State University, Leninskie gory, 1/2, Moscow, 119234, Russia;

<sup>3</sup> Department of Astrophysics and Stellar Astronomy, Physics Faculty, Lomonosov Moscow State University, Leninskie gory, 1/2, Moscow, 119234, Russia

\* Correspondence: alexeyev@sai.msu.ru

Version May 17, 2022 submitted to Universe; Typeset by L<sup>A</sup>T<sub>E</sub>X using class file mdpi.cls

**Abstract:** We review a set of the possible ways to constrain extended gravity models at Galaxy clusters scales (the regime of dark energy explanations and comparison with  $\Lambda$ CDM), for black hole shadows, gravitational wave astronomy, binary pulsars, Solar system and Large Hadron Collider (consequences for high energy physics at TeV scale). The key idea is that modern experimental and observational precise data gives a chance to go beyond the general relativity.

**Keywords:** general relativity; extended gravity; black hole; turnaround radius; shadow of black hole; gravitational waves; binary pulsars

**PACS:** 04.50.+h, 04.50.Gh, 04.80.Cc

## Contents

1	Introduction	1
2	Galaxy clusters scales: dark energy explanations	3
3	Black hole shadows: deviations from GR	4
4	Gravitational wave astronomy: deviations from GR	7
5	Binary pulsars: deviations from GR	8
6	Solar system: Newtonian limit and deviations from it	10
7	Large Hadron Collider: Constraints at TeV Scale	12
8	Conclusions	14
9	Acknowledgements	15

## 1. Introduction

The theory of General Relativity (GR) is confirmed in all projects of experimental astronomy. However the problems of dark energy, dark matter, evolution of the early Universe, quantum

theory of gravity remain open. For example, the theoretical description of the Universe accelerated expansion (i.e. dark energy) is realised by adding of the cosmological constant to the GR action  $L$  as

$$L_{GR\Lambda} = \sqrt{-g}(R + \Lambda), \quad (1)$$

where  $R$  is Ricci scalar and  $\Lambda$  is cosmological constant. The problem is that  $\Lambda$ -term is the best fit for the observational data. On the other hand from the fundamental point of view it looks as pure fine tuning parameter. The next step is to consider an additional scalar field  $\phi$  in the form of Brans-Dicke model

$$L_{BD} = \sqrt{-g} \left( \phi R + \frac{\omega}{\phi} \partial_\mu \phi \partial^\mu \phi + V(\phi) \right). \quad (2)$$

Such model can reproduce the cosmological constant contribution with the help of taking the appropriate form of  $V(\phi)$ . Now one has to find the origin of the scalar field in Eq.(2). The same problem occurs with the inflation stage: accelerated expansion of the early Universe. Mathematically the power law asymptote of scale factor is changed to exponential one. The inflation also can be modelled by the model like Eq.(2) and in such a case the scalar field is called as “inflaton”. As a consequence, one meets the question on the fundamental physical origin of inflaton. Of course, the list of such phenomenons is more wide. So the extension of GR by additional physical fields or curvature terms [1] could be the next step in finding the origin of these phenomenons.

GR extending could be proceed in different ways. One can add the curvature invariants or pure degrees of scalar curvature and obtain  $f(R)$  gravity [2]. These curvature corrections can reproduce the necessary behaviour but one meets the question on their origin once more. About ten years ago the application of Horndesky theory [3,4] (the most general form of scalar tensor gravity with second order field equations) became very popular. The successful development of Horndesky theory was corrected by GW170817 event [5]. So, a Binary Neutron Star Merger was detected. In addition to gravitational wave an electromagnetic signal was also registered. Based on the time delay (about 2 seconds) between these types of radiation arrival the graviton mass value was limited [6,7]. This limitation made a cutoff of a big class of extended gravity models where graviton mass appeared to be greater. Therefore during last years a set of beyond Horndesky models forming a class of Degenerate Higher-Order Scalar-Tensor theories (DHOST) was developed [8]. The ideas of  $f(R)$  gravity as more simple model [2] also are developed. The set of extended gravity models is more wide. We restrict ourselves by the discussion on scalar-tensor gravity models as they developed rather good and the corresponding constraints look maximally clear. Of course the list of models and corresponding constraints could be continued.

Note that now there is no preferred extended gravity model. A lot of versions in each class exist. The possible way to narrow down the amount of extended gravity models is to compare these predictions with real astrophysical data [9,10]. To extract the models giving more accurate predictions or containing less amount of fine tuning it is desirable to consider the maximally wide range of energies and distances: from galaxy clusters till high energy physics. Therefore we discuss a set of astrophysical tests for extended gravity models. Note that this list is far from being complete and represents only a small set of examples (open for extension).

We start the consideration from the scales of galaxy clusters. At these ranges the contribution of accelerated expansion (dark energy) becomes considerable. Earlier it was suggested to use the turn-around radius [11,12]. Recall that turnaround radius is a hypothetical surface where the internal gravitational force is equated by the accelerated expansion one. From one side the value of the turnaround radius could be estimated using observational data on clusters sizes. Such assumption could be obtained from gravitational lensing. From the other side this value can be directly calculated from GR. As a first approximation a spherically-symmetric space-time could be taken. Extended gravity models has different spherically-symmetric metrics so one obtains the possibility to compare the calculated values with observational ones to find the best correspondence.

The next step is to check the predictions of extended gravity models for shadows of black holes (BH). From one side the Event Horizon Telescope is providing images for M87 [13] with the increasing accuracy [14]. From the other side the shadow size, form and other characters depend on BH solution. As BH metrics are specific for each extended gravity model, here is the other possibility to compare the predictions of extended gravity models with Event Horizon Telescope observational results.

The same approach is applicable in order to find the constraints from gravitational wave astronomy [15]. The LIGO collaboration continues to collect data [16] on neutron stars and black holes mergers [17]. From the other side different extended gravity models provide different descriptions for gravitational waves. So their comparing could provide new information. Continuation of astronomical tests seems to be impossible without the most accurate data in astronomy: pulsar timing [18], especially for PSR-1913+16 [19]. The idea to use pulsar data for strong field tests of relativistic gravity [20] appeared to be very fruitful. Now it can be applied for extended gravity models. The idea is the same as previously: to reproduce the values of Post-Keplerian formalism using the specific extended gravity model parameters, then to extract the model that better reproduces the observational results [21].

The decreasing of the distances leads us to the Solar System ones. The Parametric Post-Newtonian (PPN) formalism [22] appears to be very effective to constrain different gravity models. In Solar System one has a competition between the maximal experimental accuracy versus vanishing additions to GR coming from extended gravity especially while using the last data [23].

It is impossible not to mention the ideas of gravity constraining using high energy physics data from Large Hadron Collider (LHC). The well-famous idea to search black holes at LHC [24] (and to discriminate some theories [25]) is not very popular now. Anyway LHC data help to put some limitations on gravity in quantum regime [26].

The paper is organised as follows. Section 2 is devoted to the difference of Extended Gravity predictions from General Relativity ones at Galaxy clusters scales (the regime of dark energy explanations and comparison with  $\Lambda$ CDM), Section 3 deals with black hole shadows, Section 4 is devoted to the gravitational wave astronomy, Section 5 deals with binary pulsars, Section 6 is devoted to the Solar system, Section 7 deals with consequences from experimental high energy physics at TeV scale and Section 8 includes the concluding remarks.

## 2. Galaxy clusters scales: dark energy explanations

Nowadays the  $\Lambda$ CDM model with the action

$$S = \frac{1}{16\pi} \int d^4x \sqrt{-g} (R + \Lambda), \quad (3)$$

where  $g_{\mu\nu}$  is the space-time metrics (with determinant  $g$ ),  $R$  is Ricci scalar and  $\Lambda$  is cosmological constant, being the best fit for observational data, provides a good description of dark energy. So to suggest a good physical interpretation of cosmological constant it seems useful to modify GR [27]. Therefore the models of  $f(R)$  gravity (where  $\Lambda$  is treated as a manifestation of a knotty space-time geometry), scalar-tensor ones (where in addition to the previous one deals with additional fields), modern teleparallel ones (where the complex fundamental geometry is explored) and other ideas are developing. The first step in each GR extension leads to Brans-Dicke model

$$S = \frac{1}{16\pi} \int d^4x \sqrt{-g} \left( \phi R - \frac{\omega}{\phi} g^{\mu\nu} \nabla_\mu \phi \nabla_\nu \phi - V(\phi) + L_{matter} \right), \quad (4)$$

where  $\phi$  is scalar field,  $\omega$  is Brans-Dicke parameter,  $V(\phi)$  is field potential and  $L_{matter}$  is the contribution of matter fields. The model (4) reproduces the contribution of  $\Lambda$ . On the other hand the question on the origin of  $\Lambda$  changes to the same one on  $\phi$ . That is why it is necessary to go further, for example, to  $f(R)$  gravity [28]. In the frames of  $f(R)$  gravity a very interesting model was

presented [29]. Being a good fit for  $\Lambda$  this model is called as Starobinsky model with disappearing cosmological constant. Note that further the continuation of this model appeared [30]. This approach allows to provide the unified theory both for inflation and dark energy. So the Starobinsky model with disappearing cosmological constant is described by the following Lagrange density:

$$f(R) = R + \lambda R_0 \left( \left[ 1 + \frac{R^2}{R_0^2} \right]^{-n} - 1 \right), \quad (5)$$

where  $R_0$  and  $n$  are model parameters. Using Starobinsky model with disappearing cosmological constant as an example we demonstrate how to constrain the theory at extra-galactic distances.

At the range of galaxy clusters the contribution of Universe accelerated expansion is considerable therefore the application of the turn-around radius [11,31] looks perspective. Recall that the turnaround radius is a hypothetical surface where the internal gravitational forces are equated by the accelerated expansion ones. The value of the turnaround radius estimates from observational data. Namely cluster size estimates using gravitational lensing (see, for example, [32–34]). On the other hand the value the turnaround radius can be calculated using spherically-symmetric space-time as the first approximation. Different extended gravity models result in different versions of spherically-symmetric metrics. So it is possible to compare these calculated values with observational estimations to find the best correspondence. Note that there are a lot of activity in this field, for example [35–44].

As an example we show the procedure of Starobinsky model with vanishing cosmological model check up [12]. As a first approximation it is convenient to take the metric in quasi-Schwarzschild form:

$$ds^2 = e^A dt^2 - e^{-A} dr^2 - r^2 d\Omega, \quad (6)$$

where  $A = A(r)$  is metric function (for Schwarzschild case  $A = 1 - 2M/r$ ). Here it is necessary to note that the usage of Schwarzschild metric (6) here is an approximation. Really, spherically-symmetric solutions for the extended models must have two or more metric functions [45]. As the Schwarzschild metric could be treated as first terms of the Taylor expansion correspondingly  $r^{-1}$  the application of the Schwarzschild metric here could be treated as first approximation. Formally this analysis has to be extended. We restrict this procedure because of the observational data errors. So, the corresponding field equations are [46]:

$$f'(R)R_{ii} - f(R)\frac{g_{ii}}{2} - (\nabla_i^2 - g_{ii}\square)f'(R) = 0. \quad (7)$$

At the turnaround radius the first derivative of gravitational potential

$$\phi = \frac{1}{2}(g_{00} - 1) = \frac{1}{2}(e^A - 1) \quad (8)$$

must vanish:

$$\frac{dA}{dr} = 0. \quad (9)$$

Solving Eq (9) together with Eqs (7) numerically one finds the dependence of turnaround radius versus different values of  $n$  from Eq.(5). The most interesting mass range begins from  $10^{11}M_{Sun}$  (Milky Way) and finishes at  $10^{15}M_{Sun}$  (galaxy clusters). The results are demonstrated at Fig. 1 from which one concludes that less values of  $n$  provide better approximation of observational data. The same analysis could be proceed for other extended gravity models, for example, the very rough approximation for Horndesky theory is presented in [47].

### 3. Black hole shadows: deviations from GR

The idea to use the images of BH shadows for testing of extended gravity theories develops during last 10 years [48,49]. Note that the same form of BH shadow can be obtained in the frames

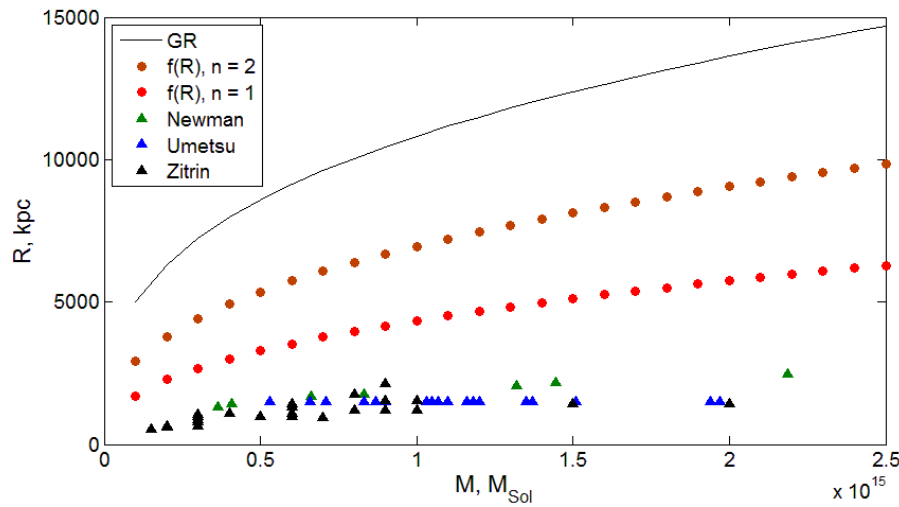


**Figure 1.** The theoretical and observational assumptions for the dependence of the turnaround radius value upon the mass of the galaxy cluster. The solid line corresponds to GR. Dots show these values for Starobinsky model with  $n = 1$  and  $n = 2$ . Triangles show the real data from [32–34]. Reproduced from [12]

of different gravity theories. As usually GR solutions (as the simplest ones) are taken as the first approximation. Note that there are a lot of activity in this field, for example [50–63]. So, a non-rotating non-charged (Schwarzschild) BH (in the Planck system of units  $G = c = \hbar = 1$ ) is described by the following metric:

$$ds^2 = -A(r)dt^2 + B(r)dr^2 + r^2(d\theta^2 + \sin^2\theta d\phi^2), \quad (10)$$

where

$$A(r) = B(r)^{-1} = 1 - \frac{2M}{r}, \quad (11)$$

$M$  is the mass of the BH. If the electromagnetic field (or new physics contribution) is taken into account, the Reissner-Nordstrom metric appears to be valid:

$$A(r) = B(r)^{-1} = 1 - \frac{2M}{r} + \frac{Q^2}{r^2}, \quad (12)$$

where  $Q$  is the electric or tidal charge. The rotation can be included with the help of the Newman-Janis algorithm[64]. Applying it to 11 one results in the Kerr-Newman metric in the form:

$$ds^2 = - \left( 1 - \frac{2m(r)r}{\rho^2} \right) dt^2 - \frac{4m(r)ar \sin^2\theta}{\rho^2} d\phi dt + \frac{\rho^2}{\Delta} dr^2 + \rho^2 d\theta^2 + \left( r^2 + a^2 + \frac{2m(r)a^2 r \sin^2\theta}{\rho^2} \right) \sin^2\theta d\phi^2, \quad (13)$$

where

$$\begin{aligned} \rho^2 &= r^2 + a^2 \cos^2\theta, \\ \Delta(r) &= r^2 - 2m(r)r + a^2, \\ m(r) &= M - \frac{Q^2}{2r}, \end{aligned} \quad (14)$$

$a = J/M$  is the BH acceleration and  $J$  is its angular momentum. If  $Q = 0$  one obtains an uncharged rotating BH described by the Kerr metric. For Reissner-Nordstrom metric ( $q \rightarrow Q^2$ ) the radius of BH shadow was calculated analytically [48] and is equal to

$$D = \sqrt{\frac{(8q^2 - 36q + 27) + \sqrt{(8q^2 - 36q + 27)^2 + 64q^3(1 - q)}}{2(1 - q)}}. \quad (15)$$

When  $q > 1$  the object has no horizon and the minimum size of the BH shadow is equal to  $4M$ . From 15 one sees that for  $q > 9/8$  a photon sphere is absent. For more complicated theories there is impossible to obtain the analytical solution. So the numerical methods must be used.

For the space-time (10) in general  $A(r) \neq -B(r)^{-1}$ . Corrections from extended theories can be represented as additional terms of the Taylor series expansion around Schwarzschild metric. Therefore to simulate the shadow one have to study the equations of motion of the photons around the BH. So,

$$u(r) = \left( \frac{d\hat{r}}{d\phi} \right)^2 = \frac{\hat{r}^4}{D^2 A(\hat{r}) B(\hat{r})} - \frac{\hat{r}^2}{B(\hat{r})}, \quad (16)$$

where  $D = L/E$  is the aiming parameter of the photon beam. The edge of the shadow corresponds to the transition of light particles to an unstable orbit. The conditions of this transition are:

$$u(r) = 0, \quad \frac{du(r)}{dr} = 0, \quad \frac{d^2 u(r)}{d^2 r} > 0 \quad (17)$$

The size of the shadow is defined by the the maximal solution of Eqs (17). The accounting of  $1/r^{-3}$  correction allows to cover the wider range of shadow sizes. For example it becomes possible to study BH shadow with the size less than  $4M$  [65,66]. Moreover the objects with a horizon but without the photon sphere become being well described. This is a BH without a shadow appearing in the models with beyond Reissner-Nordstrom metrics.

It is important to note that many theories predict the existence of BH shadows with the same size. To determine the theory type additional tests of the BH potential are required. They are, for example, strong gravitational lensing of bright objects around the BH, the last stable orbit of the accretion disk, the distribution of background intensity from ionised plasma around the BH, ... Earlier [65,66] we estimated the accuracy value that is enough to constrain extended theory in BH non-rotating case. For strong gravitational lensing this accuracy is about  $10^3$  times less than the angular size of the BH is required. For the background intensity the necessary accuracy is also  $\approx 10^3$  times less than the its maximum value.

One of the ways to include rotation is to apply the Newman-Janis algorithm [67]. The usage of  $m(r)$  term allows to incorporate various models. Generically for the corrections established as Taylor series the procedure is the following:

$$m(r) = M - \frac{q}{2r} - \frac{C_3}{2r^2} - \dots - \frac{C_n}{2r^{n-1}} - \dots \quad (18)$$

Therefore the coordinates of the shadow edge  $[\alpha, \beta]$  on the image plane are:

$$\alpha = \frac{\xi_-}{\sin \theta_i}, \quad \beta = \pm \sqrt{\eta_- + (a - \xi_-)^2 - \left( a \sin \theta_i - \frac{\xi_-}{\sin \theta_i} \right)^2}, \quad (19)$$

where  $\theta_i$  is the angle of inclination of the BH rotation axis,

$$\begin{aligned}
 \xi_- &= \frac{4r_0^2 \xi_A - (r_0^2 + a^2) \xi_B}{a \xi_C}, \\
 \eta_- &= \frac{r_0^3 [\eta_A a^2 - r_0 \eta_B^2]}{a^2 \eta_C^2}, \\
 \xi_A &= M - \frac{q}{2r_0} - \frac{C_3}{2r_0^2} - \dots - \frac{C_n}{2r_0^{n-1}} - \dots, \\
 \xi_B &= r_0 + M + \frac{C_3}{2r_0^2} + \dots + \frac{(n-2)C_n}{2r_0^{n-1}} + \dots, \\
 \xi_C &= r_0 - M - \frac{C_3}{2r_0^2} - \dots - \frac{(n-2)C_n}{2r_0^{n-1}} - \dots, \\
 \eta_A &= 4M - \frac{4q}{r_0} - \frac{6C_3}{r_0^2} - \dots - \frac{2nC_n}{r_0^{n-1}} - \dots, \\
 \eta_B &= r_0 - 3M + \frac{2q}{r_0} + \frac{5C_3}{2r_0^2} + \dots \\
 &\quad + \frac{(n+2)C_n}{2r_0^{n-1}} + \dots, \\
 \eta_C &= r_0 - M - \frac{C_3}{2r_0^2} - \dots - \frac{(n-2)C_n}{2r_0^{n-1}} - \dots,
 \end{aligned} \tag{20}$$

For the corrections in the form of Taylor expansion the accuracy was estimated earlier [68] where the shapes of BH shadows with the same size have been compared. The deviation of the shape from the Kerr BH one reaches 2% of the shadow size (Fig.2) for the expansions up to  $r^{-3}$ , strong rotation with  $a = 0.9$  and for  $q$  and  $C_3$  comparable with  $M$  (for example,  $q = 0.17$ ,  $C_3 = -0.5$ ). To constrain rapidly rotating BH the accuracy an order of magnitude better is required. This is about hundred times louder than the size of the shadow.

As a result: in order to test gravity theories one needs the resolution being hundreds times better than was reached in [13]. The current radio telescopes are already used in one big web. So the next step to improve the resolution is to use space telescopes.

#### 4. Gravitational wave astronomy: deviations from GR

One of the most well-known results in experimental astronomy is the registration of gravitational waves [69]. From the mathematical point of view the gravitational wave is a solution of GR and the existing experimental results completely correspond to it. The LIGO collaboration continues to collect data [16] on neutron stars and black holes mergers [17]. The most interesting event for our aims is GW170817 [70] when two neutron stars merged not far from us. Thanks to this the direction to the source was discovered. So the corresponding electromagnetic signal was also registered [71]. The time delay between gravitational and electromagnetic signals was equal to 1.6 seconds. Such value of time delay puts a strong limitation on graviton mass [6]. Therefore it makes a great cutoff for the models of massive gravity. Based on this data graviton mass appears to be less than  $10^{-22} \text{ eV}$ . Hence, the difference between the speeds of light and gravitational wave could not be more than  $1 + 10^{-16}$ . Such a restriction excludes a big set of models with massive graviton (and, therefore, models where it could appear). After GW170817 such models as quartic/quintic galileons, models Fab Four (for additional clarifications see [72]), some Degenerated Higher Order Scalar Tensor



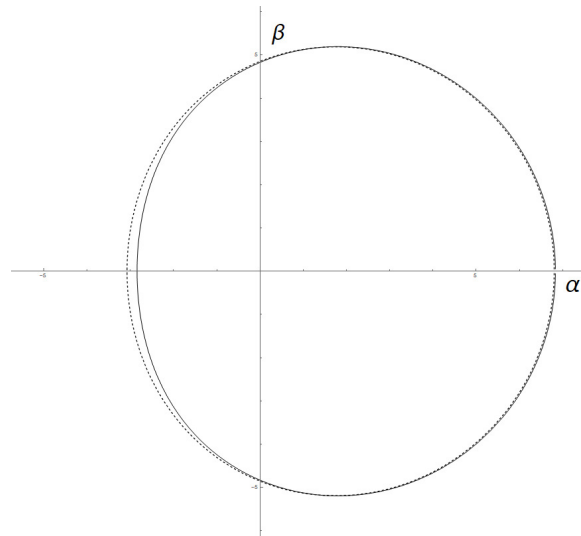


**Figure 2.** Black holes with the spin equal to  $a = 0.9$  and the following parameters: dashed line corresponds to  $q = 0.17$ ,  $C_3 = -0.5$ , solid one corresponds to  $q = 0$ ,  $C_3 = 0$ . The rotation axis is directed along the  $\beta$  one, the inclination angle is equal to  $\theta_i = -\pi/2$ . Reproduced from [68]

(DHOST) models with  $A_1 \neq 0$  and many others appeared to be excluded [6,7]. Horndesky models (as general version of scalar-tensor gravity with second order field equations [3,4]) being for a long time the top candidate for dark energy and dark matter explanations after GW170817 are restricted as  $G_{4,X} = 0$ ,  $G_5 = \text{const}$  [6]. Therefore to follow GW170817 limit a new set of models namely beyond Horndesky was developed. There are such theories as derivative conformal models, models with disformal tuning and DHOST models with  $A_1 = 0$  and so on [6,7]. Of course, more simple theories as Brans-Dicke and  $f(R)$  models remain in use. Finally each viable gravitational model must pass the gravitational wave astronomy tests (including LIGO-VIRGO last runs).

Note that the subject of how gravitational wave astronomy could constrain extended gravity models is much more wide. We restrict our consideration with GW170817 test as it seems to be most intriguing. One can extend the discussion, for example, by the notes on the forms of gravitational wave solutions in different models and the number of polarisation modes.

## 5. Binary pulsars: deviations from GR

Any discussion on astronomical tests would be incomplete without mentioning of the most accurate astrophysical data set: pulsar timing [18]. The most accurate data is provided by PSR-1913+16 [19]. The key idea remains the same: to reproduce all Post-Keplerian parameters using the specific extended gravity model. Then one has to find the model which covers the observational results better [21]. Note that in binary pulsars one deals with the gravitational field much stronger than in Solar system. It lies closer to the one discussed in the previous section. Thanks to the stability of the pulse signal one can extract the orbital motion dynamics and gravitational waves emission contributions. There are a lot of activity in this field, for example [6,9,73,74].

Following [20,75,76] we start from the famous timing formula:

$$t_B - t_0 = D^{-1} \left[ T + \Delta_R(T, \dot{\omega}, \dot{P}_b, \delta_r, \delta_\theta) + \Delta_E(T, \gamma) + \Delta_S(T, r, s) + \Delta_A(T, A, B) \right], \quad (21)$$

where  $t_B$  is time of arrival of an impulse at the barycenter of the solar system,  $t_0$  is observable time of impulse arriving,  $D$  is the Doppler factor,  $T$  is the time of impulse emission, ( $\Delta_R$ ,  $\Delta_E$ ,  $\Delta_S$  and  $\Delta_A$ ) are the propagation delays due to “Roemer”, “Einstein”, “Shapiro” (see, in addition, [77])



and “aberration” effects respectively. These delays depend upon the parametrized keplerian and post-keplerian (PPK) parameters ( $\omega$ ,  $P_b$ ,  $\delta_r$ ,  $\delta_\theta$ ,  $\gamma$ ,  $r$ ,  $s$ ,  $A$ ,  $B$ ) are periastron longitude, pulsar orbital period and its first derivative, two parameters of orbit deformation, Einstein delay, two parameters of Shapiro delay, two aberration parameters. The strategy of these values calculation is presented in lots of papers following the original Damour & Taylor ones. It is important to emphasize that these PPK parameters are calculated using metric decomposition and power series. Hence the result for each model is unique. The ideas to constrain extended gravity models were developed [78] and it was shown that GR ideally passes through  $(\dot{P}_b - \dot{\omega} - \gamma)$  test if the existence of gravitational waves is taken into account.

Let's concentrate on  $\dot{P}_b$  version. In [21] its form was calculated for the general version of scalar-tensor gravity, i.e. Horndesky model. So, the  $\dot{P}_b^{th}/\dot{P}_b^{GR}$  relation where  $\dot{P}_b^{th}$  is the first derivative of the orbital period for the theory under consideration and  $\dot{P}_b^{GR}$  is the same value for GR can be established as:

$$\begin{aligned} \frac{\dot{P}_b^{th}}{\dot{P}_b^{GR}} = & \frac{\mathcal{G}_{12}^{\frac{2}{3}}}{G^{\frac{5}{3}}G_{4(0,0)}} \left\{ 1 + \frac{5G_{4(1,0)}c_\varphi}{48} \left( \frac{P_b c^3}{2\pi m \mathcal{G}_{12}} \right)^{\frac{2}{3}} \times \left[ A_d^2 + \frac{2\mu}{c^2} A_d \bar{A}_d \left( \frac{4\pi^2}{P_b^2 m \mathcal{G}_{12}} \right)^{\frac{1}{3}} \right] \left( 1 - \frac{m_\varphi^2 c^2 P_b^2}{4\pi^2} \right)^{\frac{3}{2}} \right. \\ & \left. + \frac{G_{4(1,0)}c_\varphi}{3} A_d^2 \left( 1 - \frac{m_\varphi^2 c^2 P_b^2}{16\pi^2} \right)^{\frac{5}{2}} - \frac{G_{4(1,0)}c_\varphi}{96} A_d A_o \left( 1 - \frac{m_\varphi^2 c^2 P_b^2}{4\pi^2} \right)^{\frac{5}{2}} \right\}, \end{aligned} \quad (22)$$

where  $\dot{P}_b^{GR}$  is:

$$\dot{P}_b^{GR} = -\frac{192\pi\mu}{5c^5 m} \left( \frac{2\pi G m}{P_b} \right)^{\frac{5}{3}}, \quad (23)$$

$G(i, j)$  are the part of Horndesky model [3,4] and  $P_b$  is the standard expression for the orbital period. Based on Eq. (22) and using the real data from PSRJ1738 + 0333 one can calculate constraints on different extended gravity models. So the key formula allowing to calculate the limitations on the considered model is

$$\left| \frac{\dot{P}_b^{th}}{\dot{P}_b^{GR}} - \frac{\dot{P}_b^{obs}}{\dot{P}_b^{GR}} \right| \leq 2\sigma, \quad (24)$$

where  $\sigma$  is the observational uncertainty and  $\dot{P}_b^{obs}/\dot{P}_b^{GR}$  is the observational quantity at 95% confidence level.

The first example is massive scalar-tensor gravity. Substituting its specific values and PSR J1738+0333 data to the Eq. (24) one obtains that

$$\left| \frac{\mathcal{G}_{12}^{\frac{2}{3}}}{G^{\frac{5}{3}}G_{4(0,0)}} \left[ 1 + \frac{5c_\varphi}{12} \left( \frac{P_b c^3}{2\pi m \mathcal{G}_{12}} \right)^{\frac{2}{3}} \left( 1 - \frac{m_\varphi^2 c^2 P_b^2}{4\pi^2} \right)^{\frac{3}{2}} \times \left( \frac{G_{4(0,0)}^2 (s_{NS} - s_{WD})^2}{G_{4(1,0)} \phi_0^2} \right) \right] - 0.93 \right| \leq 0.26. \quad (25)$$

Here  $s_{NS}$  is sensitivity of neutron star and  $s_{WD}$  is the sensitivity of white dwarf. So one obtains the upper boundary for the scalar field mass  $m_\varphi$ :

$$m_\varphi < 7 \times 10^{-15} (\text{cm}^{-1}). \quad (26)$$

The second example is hybrid metric-Palatini  $f(R)$  gravity. This model is developed as a mixture of metric and Palatini formalisms. The aim is to use the approach providing the best theoretical description in the considered range. For example the hybrid  $f(R)$ -gravity describes the accelerated

Universe expansion without introducing of new degrees of freedom. Using the set of transfer parameters [21] one obtains that

$$0.67 \leq \frac{1}{(1 + \phi_0)^{\frac{5}{3}}} \left( 1 - \frac{5\phi_0}{18} (1 - 3 \times 10^{27} m_\phi^2) \right) \leq 1, \quad (27)$$

where the dependence of the scalar field mass upon scalar field background value for PSR J1738+0333 can be taken from [21]. So the combined restrictions from  $\gamma_{PPN}$  and system PSR J1738+0333 are:

$$\phi_0 \leq 0.00004, \quad m_\phi \leq 1.4 \times 10^{-14} (\text{cm}^{-1}). \quad (28)$$

The consideration could be extended [79] to constrain other theories.

## 6. Solar system: Newtonian limit and deviations from it

Solar System contains a set of small parameters. They are, for example, Newtonian potential, matter velocity relatively the mass centre, ... So, these values could be used as expansion parameters to consider the Taylor expansion of the metric. The standardised expansion represent PPN with the coefficients measured experimentally. We shall not discuss PPN formalism in detail as there are a lot of beautiful reviews (see, for example, [80]) and textbooks ([22]). Here we show the usage of PPN to constrain the hybrid metric-Palatini gravity.

The hybrid metric-Palatini  $f(R)$ -gravity is a part of  $f(R)$ -theories [2,81]. Indeed there are two ways to obtain field equations: the metric one and the Palatini one. In the metric approach the metric  $g_{\mu\nu}$  is treated as the unique dynamical variable. The Palatini method supposes the Riemann curvature tensor as independent upon the metric and dependent only upon connection. So, variations with respect to the metric and the connection become independent. Both gravity models, i.e. metric one and Palatini one cause problems. The metric  $f(R)$ -gravity in general case does not pass the standard Solar System tests [82–84]. Palatini  $f(R)$  models contain microscopic matter instabilities [85,86]. In order to cancel these pathologies in both metric and Palatini formulations the hybrid metric-Palatini  $f(R)$ -gravity was developed [87,88]. This model combines the GR Lagrangian and the  $f(\mathfrak{R})$ -term constructed by the Palatini formalism. Therefore, all results obtained in the frames of GR are covered by the  $R$  part and  $f(\mathfrak{R})$  part is responsible for unexplained gravitational phenomena.

Further the hybrid  $f(R)$ -gravity can be established as a scalar-tensor theory [87,88]. If the appearing scalar field would be light enough it could modify the cosmological and galactic dynamics to cover unexplained phenomena leaving the Solar System unaffected. So it appears to be possible to provide a test of the hybrid  $f(R)$ -theory in the weak-field limit using the modified PPN formalism.

We start from the action [23,87,88]

$$S = \frac{c^4}{2k^2} \int d^4x \sqrt{-g} [R + f(\mathfrak{R})] + S_m, \quad (29)$$

where  $c$  is the speed of light,  $k^2 = 8\pi G$ ,  $R$  and  $\mathfrak{R} = g^{\mu\nu} \mathfrak{R}_{\mu\nu}$  are the metric and Palatini curvatures respectively,  $g$  is the metric determinant,  $S_m$  is the matter action. The Palatini curvature  $\mathfrak{R}$  is considered depending upon  $g_{\mu\nu}$  and the independent connection  $\hat{\Gamma}_{\mu\nu}^\alpha$ :

$$\mathfrak{R} = g^{\mu\nu} \mathfrak{R}_{\mu\nu} = g^{\mu\nu} (\hat{\Gamma}_{\mu\nu,\alpha}^\alpha - \hat{\Gamma}_{\mu\alpha,\nu}^\alpha + \hat{\Gamma}_{\alpha\lambda}^\alpha \hat{\Gamma}_{\mu\nu}^\lambda - \hat{\Gamma}_{\mu\lambda}^\alpha \hat{\Gamma}_{\alpha\nu}^\lambda). \quad (30)$$

The discussed model allows the scalar-tensor representation in the Jordan frame in the form

$$S = \frac{c^4}{2k^2} \int d^4x \sqrt{-g} \left[ (1 + \phi) R + \frac{3}{2\phi} \partial_\mu \phi \partial^\mu \phi - V(\phi) \right] + S_m, \quad (31)$$

where  $\phi$  is a scalar field and  $V(\phi)$  is its potential. The following field equations are:

$$(1 + \phi)R_{\mu\nu} = \frac{k^2}{c^4} \left( T_{\mu\nu} - \frac{1}{2} g_{\mu\nu} T \right) + \frac{1}{2} g_{\mu\nu} \left[ V(\phi) + \nabla_\alpha \nabla^\alpha \phi \right] + \nabla_\mu \nabla_\nu \phi - \frac{3}{2\phi} \partial_\mu \phi \partial_\nu \phi, \quad (32)$$

$$\nabla_\mu \nabla^\mu \phi - \frac{1}{2\phi} \partial_\mu \phi \partial^\mu \phi - \frac{\phi[2V(\phi) - (1 + \phi)V_\phi]}{3} = -\frac{k^2}{3c^4} \phi T. \quad (33)$$

Here it is necessary to note that the scalar field is dynamical in the hybrid  $f(R)$ -gravity. So, there are no microscopic instabilities associated with in pure Palatini models.

We start from expanding of the scalar  $\phi$  and the tensor  $g_{\mu\nu}$  fields as

$$\phi = \phi_0 + \varphi, \quad g_{\mu\nu} = \eta_{\mu\nu} + h_{\mu\nu}, \quad (34)$$

where  $\phi_0$  is the field asymptotic value,  $\eta_{\mu\nu}$  is the Minkowski space-time,  $h_{\mu\nu}$  and  $\varphi$  are the small perturbations of tensor and scalar fields respectively. In general  $\phi_0$  depends upon time. This dependence can be neglected if one deals with short period associated with the observational time in comparison with cosmological time scale. So, we treat  $\phi_0$  as a constant.

The PPN operates with the following orders of metric and field [22]:

$$\begin{aligned} h_{00} &\sim O(2) + O(4), \\ h_{0j} &\sim O(3), \\ h_{ij} &\sim O(2) \\ \varphi &\sim O(2) + O(4). \end{aligned}$$

Further, the Taylor expansion for the scalar potential  $V(\phi)$  around the background value  $\phi_0$  has the form:

$$V(\phi) = V_0 + V' \varphi + \frac{V'' \varphi^2}{2!} + \frac{V''' \varphi^3}{3!}. \quad (35)$$

The stress-energy tensor for point-mass gravitational systems is defined as

$$T^{\mu\nu} = \frac{c}{\sqrt{-g}} \sum_a m_a \frac{u^\mu u^\nu}{u^0} \delta^3(\vec{r} - \vec{r}_a), \quad (36)$$

where  $m_a$  is the mass of the  $a$ -th particle,  $\vec{r}_a$  is its radius-vector,  $u^\mu = dx_a^\mu/d\tau_a$  is its four-velocity,  $d\tau = \sqrt{-ds^2}/c$ ,  $ds^2 = g_{\mu\nu} dx^\mu dx^\nu$  is an interval,  $u_\mu u^\mu = -c^2$ , and  $\delta^3(\vec{r} - \vec{r}_a(t))$  is the 3D Dirac delta function. In the PPN approximation these components (36) and the trace  $T$  have the following form:

$$T_{00} = c^2 \sum_a m_a \delta^3(\vec{r} - \vec{r}_a) \left[ 1 - \frac{3}{2} h_{00} + \frac{1}{2} \frac{v_a^2}{c^2} - \frac{1}{2} h \right], \quad (37)$$

$$T_{0i} = -c \sum_a m_a v_a^i \delta^3(\vec{r} - \vec{r}_a), \quad (38)$$

$$T_{ij} = \sum_a m_a v_a^i v_a^j \delta^3(\vec{r} - \vec{r}_a), \quad (39)$$

$$T = -c^2 \sum_a m_a \delta^3(\vec{r} - \vec{r}_a) \left[ 1 - \frac{1}{2} h_{00} - \frac{1}{2} \frac{v_a^2}{c^2} - \frac{1}{2} h \right], \quad (40)$$

where  $v_a$  is the velocity of the  $a$ -th particle. At next step one uses the Nutku gauge conditions [89]:

$$h_{\beta,\alpha}^\alpha - \frac{1}{2} \delta_\beta^\alpha h_{\mu,\alpha}^\mu = \frac{\varphi_{,\beta}}{1 + \phi_0}. \quad (41)$$

After solving the correspondent field equations [23] and assuming that the main contribution comes from the Sun one obtains (here we restrict ourselves by the second order expressions because of their length) the solution for  $h_{00}^{(2)}$ :

$$h_{00}^{(2)} = \frac{k^2}{4\pi(1+\phi_0)c^2} \frac{M}{r} \left(1 - \frac{\phi_0}{3} \exp[-m_\varphi r]\right) + \frac{V_0}{1+\phi_0} \frac{r^2}{6}, \quad (42)$$

where  $M$  is the Solar mass. Here  $V_0/(\phi_0 + 1)$  represents the  $\Lambda$  term negligible in Solar System scales. In the same way

$$h_{ij}^{(2)} = \frac{\delta_{ij}k^2}{4\pi(1+\phi_0)c^2} \frac{M}{r} \left(1 + \frac{\phi_0}{3} \exp[-m_\varphi r]\right) - \delta_{ij} \frac{V_0}{1+\phi_0} \frac{r^2}{6}. \quad (43)$$

After comparing the result expressions with the general point-mass form introduced by K. Nordtvedt the expression for effective PPN parameter  $\gamma^{\text{eff}}$  can be expressed as

$$\gamma^{\text{eff}} = \frac{1 + \phi_0 \exp[-m_\varphi r]/3}{1 - \phi_0 \exp[-m_\varphi r]/3}. \quad (44)$$

Taking the Eq. (44) in a case of a light scalar field  $m_\varphi r \ll 1$  and using the experimental values of PPN parameters one constrains  $\phi_0$  as

$$-8 \times 10^{-5} < \phi_0 < 7 \times 10^{-5} \quad (45)$$

from the  $\gamma^{\text{exp}}$  at the  $2\sigma$  confidence level.

## 7. Large Hadron Collider: Constraints at TeV Scale

The last possibility to constrain extended gravity models that we discuss is the usage of high energy physics data. Following [26] we intend to demonstrate how one could constrain extended gravity model at the quantum gravity regime using LHC data.

We have no experimental data on matter properties at Planckian scale now. From the theoretical considerations it seems that the combination of Quantum Mechanics and GR may lead to a more complicated structure of space-time at short distances. So a new fundamental value as minimal length appears. Following the logic of Quantum Mechanic with uncertainty relation one concludes that it is impossible to measure distances with a precision better than the Planck length  $l_P = \sqrt{\hbar G/c^3}$  where  $\hbar$  is the Planck constant,  $G$  is gravitational constant and  $c$  is the speed of light in vacuum. Using the LHC data it appears possible to show that the scale of non-locality could actually be much larger than  $l_P$ .

Earlier it was shown that GR coupled to a quantum field theory causes non-local effects in scalar field theories [90]. Here we explore such a model with matter including spinor and vector fields. Firstly it is necessary to calculate a complete set of non-local effective operators at order  $NG^2$  where  $N = N_s + 3N_f + 12N_V$ ,  $N_s$ ,  $N_f$  and  $N_V$  denote the number of scalar, spinor, and vector fields respectively. After one could obtain a possibility to constrain the scale of space-time non-locality with the help of recent data from the LHC. So following [26] we start from perturbative linearized GR coupled to matter fields. Note that perturbative unitarity can be broken below the reduced Planck mass but it can be recovered by the accurate resummation of a series of graviton vacuum polarization diagrams in the large  $N$  limit. The key feature of this large  $N$  resummation is following. If one could keep  $NG$  small, therefore the obtained graviton propagator ( $\mu$  is the renormalization scale)

$$iD^{\alpha\beta,\mu\nu}(q^2) = \frac{i(L^{\alpha\mu}L^{\beta\nu} + L^{\alpha\nu}L^{\beta\mu} - L^{\alpha\beta}L^{\mu\nu})}{2q^2 \left(1 - \frac{NGq^2}{120\pi} \log\left(-\frac{q^2}{\mu^2}\right)\right)}, \quad (46)$$

includes some of the non-perturbative effects of quantum gravity. There are additional poles beyond the usual one at  $q^2 = 0$ . These complex poles are a sign of strong interactions and the mass and

width of these objects can be calculated. These poles being complex could have an incorrect sign between mass and width. Therefore this pole could be associated with a particle propagating backwards in time leading to violation of causality. With the help of the in-in formalism [91,92] the causality restores. As a consequence non-local effects at the scale  $(120\pi/GN)^{1/2}$  arise. So the scale of non-locality grows. It becomes larger than  $l_P$  if there are many fields in the matter sector ( $N$  is large).

Earlier [90] it was demonstrated that the resummation of graviton propagator in Eq. (46) leads to non-local effects in scalar field theories at the range of  $(120\pi/GN)^{1/2}$ . Such consideration should be extended to spinor and vector fields. Considering a model with an arbitrary number of scalar, spinor and vector fields one has to calculate their two-by-two scattering gravitational amplitudes taking into account the dressed graviton propagator (46). Next the leading order ( $G^2N$ ) term should be extracted to present the results in terms of effective operators.

The stress-energy tensors for the different field species with spins 0, 1/2 and 1 are taken in the form [26]

$$T_{\text{scalar}}^{\mu\nu} = \partial^\mu \phi \partial^\nu \phi - \eta^{\mu\nu} L_{\text{scalar}}, \quad (47)$$

$$T_{\text{fermion}}^{\mu\nu} = \frac{i}{4} \bar{\psi} \gamma^\mu \nabla^\nu \psi + \frac{i}{4} \bar{\psi} \gamma^\nu \nabla^\mu \psi - \frac{i}{4} \nabla^\mu \bar{\psi} \gamma^\nu \psi - \frac{i}{4} \nabla^\nu \bar{\psi} \gamma^\mu \psi - \eta^{\mu\nu} L_{\text{fermion}}, \quad (48)$$

$$T_{\text{vector}}^{\mu\nu} = -F^{\mu\sigma} F^\nu{}_\sigma + m^2 A^\mu A^\nu - \eta^{\mu\nu} L_{\text{vector}}, \quad (49)$$

where the free field matter Lagrangians are:

$$L_{\text{scalar}} = \frac{1}{2} (\partial\phi)^2 - \frac{1}{2} m^2 \phi^2, \quad (50)$$

$$L_{\text{fermion}} = \frac{i}{2} \bar{\psi} \gamma^\sigma \nabla_\sigma \psi - \frac{i}{2} \nabla_\sigma \bar{\psi} \gamma^\sigma \psi - m \bar{\psi} \psi, \quad (51)$$

$$L_{\text{vector}} = -\frac{1}{4} F^2 + \frac{1}{2} m^2 A^2. \quad (52)$$

The non-local operators at order  $NG^2$  with scalar field look like<sup>1</sup>:

$$O_{\text{scalar},1} = \frac{NG^2}{30\pi} \partial_\mu \phi \partial_\nu \phi \ln \left( \frac{\square}{\mu^2} \right) \partial^\mu \phi' \partial^\nu \phi',$$

...

The non-local operators with spinor fields are

$$O_{\text{fermion},1} = \frac{NG^2}{60\pi} \left( \frac{i}{2} \bar{\psi} \gamma^\mu \nabla^\nu \psi - \frac{i}{2} \nabla^\mu \bar{\psi} \gamma^\nu \psi \right) (\delta_\mu^\alpha \delta_\nu^\beta + \delta_\mu^\beta \delta_\nu^\alpha) \ln \left( \frac{\square}{\mu^2} \right) \left( \frac{i}{2} \bar{\psi}' \gamma^\alpha \nabla^\beta \psi' - \frac{i}{2} \nabla^\alpha \bar{\psi}' \gamma^\beta \psi' \right),$$

...

The non-local operators involving vector fields only are:

$$O_{\text{vector},1} = \frac{NG^2}{30\pi} (F^{\mu\sigma} F_{\nu\sigma} - m^2 A^\mu A_\nu) \ln \left( \frac{\square}{\mu^2} \right) (F'^{\mu\rho} F'_{\nu\rho} - m'^2 A'_\mu A'^\nu),$$

...

<sup>1</sup> because of their length we present only one operator in each group, the other ones have the same structure, the complete set can be taken from [26]

The non-local operators involving amplitudes with scalar and vector fields only are given by

$$O_{\text{scalar-vector},1} = -\frac{NG^2}{30\pi} \partial^\mu \phi \partial_\nu \phi \ln\left(\frac{\square}{\mu^2}\right) (F_{\mu\sigma} F^{\nu\sigma} - m_A^2 A_\mu A^\nu),$$

...

The non-local operators involving amplitudes with scalar and spinor fields only are:

$$O_{\text{scalar-fermion},1} = \frac{NG^2}{30\pi} \partial_\mu \phi \partial_\nu \phi \ln\left(\frac{\square}{\mu^2}\right) \left( \frac{i}{2} \bar{\psi} \gamma^\mu \nabla^\nu \psi - \frac{i}{2} \nabla^\mu \bar{\psi} \gamma^\nu \psi \right),$$

...

The non-local operators involving amplitudes with spinor and vector fields only are:

$$O_{\text{vector-fermion},1} = -\frac{NG^2}{30\pi} \left( \frac{i}{2} \bar{\psi} \gamma^\mu \nabla^\nu \psi - \frac{i}{2} \nabla^\mu \bar{\psi} \gamma^\nu \psi \right) \ln\left(\frac{\square}{\mu^2}\right) (F_{\mu\sigma} F_\nu{}^\sigma - m_A^2 A_\mu A_\nu),$$

...

The given effective operators contain non-local part in the form of  $\ln(\square/\mu^2)$  term in the matter sector. Its extension corresponds to the minimal length that can be tested. So the space-time is smeared on distances shorter than  $M_\star = M_P \sqrt{120\pi/N}$  which corresponds to the energy of the complex pole. Therefore there is no correct definition of the space-time on distances smaller than  $1/M_\star$ . Note that the non-local effects in the four-fermion interactions can be constrained using LHC data. The ATLAS collaboration looked for four-fermion contact interactions at  $\sqrt{s} = 8$  TeV and obtained lower limits on the scale on the lepton-lepton-quark-quark contact interaction  $\Lambda$  between 15.4 TeV and 26.3 TeV [93]. The conservative approach suggests to identify the scale generated with the derivatives in the four-fermion operators with the centre of mass energy of the proton-proton collision. Therefore the conservative bound could be taken as  $N < 5 \times 10^{61}$  on the number of light fields in a hidden sector. As a result the scale  $M_\star$  (a character value of space-time non-locality) appears to be larger than  $3 \times 10^{-11}$  GeV.

## 8. Conclusions

We briefly review the set of possibilities to constrain extended gravity models at different space-time and energy scales. The key idea is to apply modern astrophysical and high energy physics data starting from big scales and to do down along the scale paying attention on common features of all mentioned items. It is importantly to note that we briefly discuss a set in a unified way, to help one to study carefully each item references to corresponding reviews are provided.

First possibility occurs at the scales of galaxy clusters where the contribution of accelerated expansion (dark energy) becomes considerable. We focused on the turn-around radius usage. Extended gravity models has different spherically-symmetric metrics so one obtains the possibility to compare the calculated values with observational ones to find the best correspondence. We showed that for Starobinsky model with the vanishing cosmological constant less values of parameter  $n$  provide better approximation for the observational data. For Horndesky model the upper limit on effective cosmological constant value is  $\Lambda_{eff} < 1.6 \cdot 10^{-48} \text{ m}^{-2}$  [47].

The next possibility to check the predictions of extended gravity models comes from shadows of black holes (BH). As we show in order to test gravity theories one needs to increase the resolution for 2 orders of magnitude than was reached in [13].

The next possibility comes from gravitational wave astronomy. We mentioned that Horndesky models after GW170817 were restricted as  $G_{4,X} = 0$ ,  $G_5 = \text{const}$  so beyond Horndesky models began active developing. Note that such theories as derivative conformal models, models with disformal tuning and DHOST models with  $A_1 = 0$  remain valid.

The next possibility is given by the most accurate data in astronomy: pulsar timing, especially for PSR-1913+16. For massive scalar-tensor gravity one obtains the upper boundary for the scalar field mass:  $m_\phi < 7 \times 10^{-15} (\text{cm}^{-1})$ . For hybrid metric-Palatini  $f(R)$  gravity this looks as  $\phi_0 \leq 0.00004$ ,  $m_\phi \leq 1.4 \times 10^{-14} (\text{cm}^{-1})$ .

The next possibility appears at the Solar System scales. For hybrid metric-Palatini  $f(R)$  gravity in a case of a light scalar field  $m_\phi r \ll 1$  and using the experimental values of PPN parameters one constrains  $\phi_0$  as  $-8 \times 10^{-5} < \phi_0 < 7 \times 10^{-5}$  from the  $\gamma^{\text{exp}}$  at the  $2\sigma$  confidence level.

The last possibility that we mention here is the idea of gravity constraining using high energy physics data from Large Hadron Collider (LHC). Here it is interesting to use ATLAS data for four-fermion contact interactions at  $\sqrt{s} = 8$  TeV and obtained lower limits on the scale on the lepton-lepton-quark-quark contact interaction  $\Lambda$  between 15.4 TeV and 26.3 TeV. Therefore the scale  $M_*$  (a character value of space-time non-locality) appears to be larger than  $3 \times 10^{-11}$  GeV.

Of course, this list is far from being complete and only few examples were demonstrated. As the accurateness of experiments and observations continues to grow new possibilities could arise in the near future.

## 9. Acknowledgements

The paper represents the extended version of the lecture presented by SA at XXII International Meeting “Physical Interpretations of Relativity Theory-2021” (July 5-9, 2021) held in Bauman Moscow State Technical University.

This research has been supported by the Interdisciplinary Scientific and Educational School of Moscow University “Fundamental and Applied Space Research”.

**Conflicts of Interest:** The authors declare no conflict of interest.

## References

1. Capozziello, S.; De Laurentis, M. Extended Theories of Gravity. *Phys. Rept.* **2011**, *509*, 167–321, [arXiv:gr-qc/1108.6266].
2. De Felice, A.; Tsujikawa, S.  $f(R)$  theories. *Living Rev. Rel.* **2010**, *13*, 3, [arXiv:gr-qc/1002.4928].
3. Horndeski, G.W. Second-order scalar-tensor field equations in a four-dimensional space. *Int. J. Theor. Phys.* **1974**, *10*, 363–384.
4. Kobayashi, T. Horndeski theory and beyond: a review. *Rept. Prog. Phys.* **2019**, *82*, 086901, [arXiv:gr-qc/1901.07183].
5. Abbott, B.P.; others. Gravitational Waves and Gamma-rays from a Binary Neutron Star Merger: GW170817 and GRB 170817A. *Astrophys. J. Lett.* **2017**, *848*, L13, [arXiv:astro-ph.HE/1710.05834].
6. Ezquiaga, J.M.; Zumalacárregui, M. Dark Energy After GW170817: Dead Ends and the Road Ahead. *Phys. Rev. Lett.* **2017**, *119*, 251304, [arXiv:astro-ph.CO/1710.05901].
7. Baker, T.; Bellini, E.; Ferreira, P.G.; Lagos, M.; Noller, J.; Sawicki, I. Strong constraints on cosmological gravity from GW170817 and GRB 170817A. *Phys. Rev. Lett.* **2017**, *119*, 251301, [arXiv:astro-ph.CO/1710.06394].
8. Ageeva, Y.; Petrov, P.; Rubakov, V. Nonsingular cosmological models with strong gravity in the past. *Phys. Rev. D* **2021**, *104*, 063530, [arXiv:hep-th/2104.13412].
9. Berti, E.; others. Testing General Relativity with Present and Future Astrophysical Observations. *Class. Quant. Grav.* **2015**, *32*, 243001, [arXiv:gr-qc/1501.07274].
10. Borka, D.; Jovanović, V.B.; Capozziello, S.; Zakharov, A.F.; Jovanović, P. Estimating the Parameters of Extended Gravity Theories with the Schwarzschild Precession of S2 Star. *Universe* **2021**, *7*, 407, [arXiv:gr-qc/2111.00578].
11. Chernin, A.D.; Emelianov, N.V.; Karachentsev, I.D. Dark energy domination in the local flow of giant galaxies. *Mon. Not. Roy. Astron. Soc.* **2015**, *449*, 2069–2078, [arXiv:astro-ph.CO/1508.03485].
12. Alexeyev, S.O.; Latosh, B.N.; Echeistov, V.A. Searching for Constraints on Starobinsky’s Model with a Disappearing Cosmological Constant on Galaxy Cluster Scales. *J. Exp. Theor. Phys.* **2017**, *125*, 1083–1089.



13. Akiyama, K.; others. First M87 Event Horizon Telescope Results. I. The Shadow of the Supermassive Black Hole. *Astrophys. J. Lett.* **2019**, *875*, L1, [[arXiv:astro-ph.GA/1906.11238](#)].
14. Kocherlakota, P.; others. Constraints on black-hole charges with the 2017 EHT observations of M87\*. *Phys. Rev. D* **2021**, *103*, 104047, [[arXiv:gr-qc/2105.09343](#)].
15. Will, C.M. Testing gravity using space gravitational-wave detectors. *Class. Quant. Grav.* **2003**, *20*, S219–S225.
16. Abbott, R.; others. All-sky search for short gravitational-wave bursts in the third Advanced LIGO and Advanced Virgo run. *Phys. Rev. D* **2021**, *104*, 122004, [[arXiv:gr-qc/2107.03701](#)].
17. Abbott, R.; others. Observation of Gravitational Waves from Two Neutron Star–Black Hole Coalescences. *Astrophys. J. Lett.* **2021**, *915*, L5, [[arXiv:astro-ph.HE/2106.15163](#)].
18. Weisberg, J.M.; Taylor, J.H. Observations of Post-Newtonian Timing Effects in the Binary Pulsar PSR 1913+16. *Phys. Rev. Lett.* **1984**, *52*, 1348–1350.
19. Hulse, R.A.; Taylor, J.H. Discovery of a pulsar in a binary system. *Astrophys. J. Lett.* **1975**, *195*, L51–L53.
20. Damour, T.; Taylor, J.H. Strong field tests of relativistic gravity and binary pulsars. *Phys. Rev. D* **1992**, *45*, 1840–1868.
21. Dyadina, P.I.; Avdeev, N.A.; Alexeyev, S.O. Horndeski gravity without screening in binary pulsars. *Mon. Not. Roy. Astron. Soc.* **2019**, *483*, 947–963, [[arXiv:astro-ph.HE/1811.05393](#)].
22. Will, C.M. *Theory and Experiment in Gravitational Physics*; Cambridge University Press, 2018.
23. Dyadina, P.I.; Labazova, S.P.; Alexeyev, S.O. Post-Newtonian Limit of Hybrid Metric-Palatini  $f(R)$ -Gravity. *J. Exp. Theor. Phys.* **2019**, *129*, 838–848.
24. Landsberg, G. Black Holes at the Large Hadron Collider. *Fundam. Theor. Phys.* **2015**, *178*, 267–292.
25. Barrau, A.; Grain, J.; Alexeyev, S.O. Gauss-Bonnet black holes at the LHC: Beyond the dimensionality of space. *Phys. Lett. B* **2004**, *584*, 114, [[hep-ph/0311238](#)].
26. Alexeyev, S.O.; Calmet, X.; Latosh, B.N. Gravity induced non-local effects in the standard model. *Phys. Lett. B* **2018**, *776*, 111–114, [[arXiv:hep-th/1711.06085](#)].
27. Rubakov, V.A.; Tinyakov, P.G. Infrared-modified gravities and massive gravitons. *Phys. Usp.* **2008**, *51*, 759–792, [[arXiv:hep-th/0802.4379](#)].
28. Capozziello, S.; Cardone, V.F.; Troisi, A. Reconciling dark energy models with  $f(R)$  theories. *Phys. Rev. D* **2005**, *71*, 043503, [[astro-ph/0501426](#)].
29. Starobinsky, A.A. Disappearing cosmological constant in  $f(R)$  gravity. *JETP Lett.* **2007**, *86*, 157–163, [[arXiv:astro-ph/0706.2041](#)].
30. Nojiri, S.; Odintsov, S.D. Unified cosmic history in modified gravity: from  $F(R)$  theory to Lorentz non-invariant models. *Phys. Rept.* **2011**, *505*, 59–144, [[arXiv:gr-qc/1011.0544](#)].
31. Faraoni, V. Turnaround radius in modified gravity. *Phys. Dark Univ.* **2016**, *11*, 11–15, [[arXiv:gr-qc/1508.00475](#)].
32. Newman, A.B.; Treu, T.; Ellis, R.S.; Sand, D.J.; Nipoti, C.; Richard, J.; Jullo, E. The Density Profiles of Massive, Relaxed Galaxy Clusters: I. The Total Density Over 3 Decades in Radius. *Astrophys. J.* **2013**, *765*, 24, [[arXiv:astro-ph.CO/1209.1391](#)].
33. Umetsu, K.; others. CLASH: Weak-Lensing Shear-and-Magnification Analysis of 20 Galaxy Clusters. *Astrophys. J.* **2014**, *795*, 163, [[arXiv:astro-ph.CO/1404.1375](#)].
34. Zitrin, A.; others. Hubble Space Telescope Combined Strong and Weak Lensing Analysis of the CLASH Sample: Mass and Magnification Models and Systematic Uncertainties. *Astrophys. J.* **2015**, *801*, 44, [[arXiv:astro-ph.CO/1411.1414](#)].
35. Arnold, C.; Puchwein, E.; Springel, V. Scaling relations and mass bias in hydrodynamical  $f(R)$  gravity simulations of galaxy clusters. *Mon. Not. Roy. Astron. Soc.* **2014**, *440*, 833–842, [[arXiv:astro-ph.CO/1311.5560](#)].
36. Bernal, T.; López-Corona, O.; Mendoza, S. Dynamics of clusters of galaxies with extended  $F_{(\chi)}$  gravity. *Rev. Mex. Astron. Astrofis.* **2019**, *55*, 237–254, [[arXiv:astro-ph.CO/1505.00037](#)].
37. Brax, P.; Rizzo, L.A.; Valageas, P. K-mouflage effects on clusters of galaxies. *Phys. Rev. D* **2015**, *92*, 043519, [[arXiv:astro-ph.CO/1505.05671](#)].
38. De Martino, I.  $f(R)$ -gravity model of the Sunyaev-Zeldovich profile of the Coma cluster compatible with Planck data. *Phys. Rev. D* **2016**, *93*, 124043, [[arXiv:astro-ph.CO/1605.08223](#)].

39. Ferraro, S.; Schmidt, F.; Hu, W. Cluster Abundance in  $f(R)$  Gravity Models. *Phys. Rev. D* **2011**, *83*, 063503, [[arXiv:astro-ph.CO/1011.0992](#)].
40. Li, B.; He, J.h.; Gao, L. Cluster gas fraction as a test of gravity. *Mon. Not. Roy. Astron. Soc.* **2016**, *456*, 146–155, [[arXiv:astro-ph.CO/1508.07366](#)].
41. Schmidt, F.; Vikhlinin, A.; Hu, W. Cluster Constraints on  $f(R)$  Gravity. *Phys. Rev. D* **2009**, *80*, 083505, [[arXiv:astro-ph.CO/0908.2457](#)].
42. Terukina, A.; Lombriser, L.; Yamamoto, K.; Bacon, D.; Koyama, K.; Nichol, R.C. Testing chameleon gravity with the Coma cluster. *JCAP* **2014**, *04*, 013, [[arXiv:astro-ph.CO/1312.5083](#)].
43. Terukina, A.; Yamamoto, K.; Okabe, N.; Matsushita, K.; Sasaki, T. Testing a generalized cubic Galileon gravity model with the Coma Cluster. *JCAP* **2015**, *10*, 064, [[arXiv:astro-ph.CO/1505.03692](#)].
44. Wilcox, H.; others. The XMM Cluster Survey: Testing chameleon gravity using the profiles of clusters. *Mon. Not. Roy. Astron. Soc.* **2015**, *452*, 1171–1183, [[arXiv:astro-ph.CO/1504.03937](#)].
45. Alexeev, S.O.; Pomazanov, M.V. Black hole solutions with dilatonic hair in higher curvature gravity. *Phys. Rev. D* **1997**, *55*, 2110–2118, [[hep-th/9605106](#)].
46. Sotiriou, T.P.; Faraoni, V.  $f(R)$  Theories Of Gravity. *Rev. Mod. Phys.* **2010**, *82*, 451–497, [[arXiv:gr-qc/0805.1726](#)].
47. Alexeyev, S.; Kovalkov, K. Extended gravity at galaxy cluster’s scales. *Int. J. Mod. Phys. A* **2020**, *35*, 2040057.
48. Zakharov, A.F. Constraints on a charge in the Reissner-Nordstrom metric for the black hole at the Galactic Center. *Phys. Rev.* **2014**, *D90*, 062007, [[arXiv:gr-qc/1407.7457](#)].
49. Zakharov, A.F. Constraints on tidal charge of the supermassive black hole at the Galactic Center with trajectories of bright stars. *Eur. Phys. J. C* **2018**, *78*, 689, [[arXiv:gr-qc/1804.10374](#)].
50. Becerra-Vergara, E.A.; Argüelles, C.R.; Krut, A.; Rueda, J.A.; Ruffini, R. Geodesic motion of S2 and G2 as a test of the fermionic dark matter nature of our Galactic core. *Astron. Astrophys.* **2020**, *641*, A34, [[arXiv:astro-ph.GA/2007.11478](#)].
51. Becerra-Vergara, E.A.; Argüelles, C.R.; Krut, A.; Rueda, J.A.; Ruffini, R. Hinting a dark matter nature of Sgr A\* via the S-stars. *Mon. Not. Roy. Astron. Soc.* **2021**, *505*, L64–L68, [[arXiv:astro-ph.GA/2105.06301](#)].
52. Benisty, D.; Davis, A.C. Dark energy interactions near the Galactic Center. *Phys. Rev. D* **2022**, *105*, 024052, [[arXiv:astro-ph.CO/2108.06286](#)].
53. Borka, D.; Jovanović, P.; Jovanović, V.B.; Zakharov, A.F. Constraining the range of Yukawa gravity interaction from S2 star orbits. *JCAP* **2013**, *11*, 050, [[arXiv:astro-ph.GA/1311.1404](#)].
54. Capozziello, S.; Borka, D.; Jovanović, P.; Jovanović, V.B. Constraining Extended Gravity Models by S2 star orbits around the Galactic Centre. *Phys. Rev. D* **2014**, *90*, 044052, [[arXiv:astro-ph.GA/1408.1169](#)].
55. Capozziello, S.; Lambiase, G.; Sakellariadou, M.; Stabile, A. Constraining models of extended gravity using Gravity Probe B and LARES experiments. *Phys. Rev. D* **2015**, *91*, 044012, [[arXiv:gr-qc/1410.8316](#)].
56. Cheng, X.T.; Xie, Y. Probing a black-bounce, traversable wormhole with weak deflection gravitational lensing. *Phys. Rev. D* **2021**, *103*, 064040.
57. de Martino, I.; della Monica, R.; de Laurentis, M.  $f(R)$  gravity after the detection of the orbital precession of the S2 star around the Galactic Center massive black hole. *Phys. Rev. D* **2021**, *104*, L101502, [[arXiv:gr-qc/2106.06821](#)].
58. Della Monica, R.; de Martino, I.; de Laurentis, M. Orbital precession of the S2 star in Scalar–Tensor–Vector Gravity. *Mon. Not. Roy. Astron. Soc.* **2022**, *510*, 4757–4766, [[arXiv:gr-qc/2105.12687](#)].
59. Della Monica, R.; de Martino, I. Unveiling the nature of SgrA\* with the geodesic motion of S-stars. *JCAP* **2022**, *03*, 007, [[arXiv:astro-ph.GA/2112.01888](#)].
60. Guerrero, M.; Olmo, G.J.; Rubiera-Garcia, D.; Gómez, D.S.C. Shadows and optical appearance of black bounces illuminated by a thin accretion disk. *JCAP* **2021**, *08*, 036, [[arXiv:gr-qc/2105.15073](#)].
61. Liu, T.; Zhang, X.; Zhao, W. Constraining  $f(R)$  gravity in solar system, cosmology and binary pulsar systems. *Phys. Lett. B* **2018**, *777*, 286–293, [[arXiv:astro-ph.CO/1711.08991](#)].
62. Psaltis, D.; Johannsen, T. Sgr A\*: The Optimal Testbed of Strong-Field Gravity. *J. Phys. Conf. Ser.* **2011**, *283*, 012030, [[arXiv:astro-ph.HE/1012.1602](#)].
63. Will, C.M. Testing the general relativistic no-hair theorems using the Galactic center black hole SgrA\*. *Astrophys. J. Lett.* **2008**, *674*, L25–L28, [[arXiv:astro-ph/0711.1677](#)].

64. Newman, E.T.; Janis, A.I. Note on the Kerr Spinning-Particle Metric. *Journal of Mathematical Physics* **1965**, *6*, 915–917.
65. Alexeyev, S.O.; Petrov, A.N.; Latosh, B.N. Maeda-Dadhich Solutions as Real Black Holes. *Phys. Rev.* **2015**, *D92*, 104046, [[arXiv:gr-qc/1503.06780](#)].
66. Prokopov, V.; Alexeyev, S.; Zenin, O. Black Hole Shadows: How to Fix the Extended Gravity Theory **2021**. [[arXiv:gr-qc/2107.01115](#)].
67. Tsukamoto, N. Black hole shadow in an asymptotically flat, stationary, and axisymmetric spacetime: The Kerr-Newman and rotating regular black holes. *Physical Review D* **2018**, *97*.
68. Alexeyev, S.O.; Prokopov, V.A. Shadows from spinning black holes in extended gravity. *J. Exp. Theor. Phys.* **2020**, *130*, 666–670, [[arXiv:gr-qc/2001.09272](#)].
69. Abbott, B.P.; others. Observation of Gravitational Waves from a Binary Black Hole Merger. *Phys. Rev. Lett.* **2016**, *116*, 061102, [[arXiv:gr-qc/1602.03837](#)].
70. Abbott, B.P.; others. GW170817: Observation of Gravitational Waves from a Binary Neutron Star Inspiral. *Phys. Rev. Lett.* **2017**, *119*, 161101, [[arXiv:gr-qc/1710.05832](#)].
71. Abbott, B.P.; others. Multi-messenger Observations of a Binary Neutron Star Merger. *Astrophys. J. Lett.* **2017**, *848*, L12, [[arXiv:astro-ph.HE/1710.05833](#)].
72. Latosh, B. Fab Four Effective Field Theory Treatment. *Eur. Phys. J. C*, *78*, 991, [[arXiv:gr-qc/1812.01881](#)].
73. Damour, T.; Esposito-Farese, G. Tensor - scalar gravity and binary pulsar experiments. *Phys. Rev. D* **1996**, *54*, 1474–1491, [[gr-qc/9602056](#)].
74. Creminelli, P.; Vernizzi, F. Dark Energy after GW170817 and GRB170817A. *Phys. Rev. Lett.* **2017**, *119*, 251302, [[arXiv:astro-ph.CO/1710.05877](#)].
75. Kopeikin, S.M. Supplementary Parameters in the Parameterized Post-Keplerian Formalism. *Astrophysical Journal Letters* **1994**, *434*, L67.
76. Taylor, J.H. Binary pulsars and relativistic gravity. *Rev. Mod. Phys.* **1994**, *66*, 711–719.
77. Dyadina, P.I.; Labazova, S.P. On Shapiro time delay in massive scalar-tensor theories. *JCAP* **2022**, *01*, 029, [[arXiv:gr-qc/2111.13900](#)].
78. Damour, T.; Esposito-Farese, G. Testing gravity to second postNewtonian order: A Field theory approach. *Phys. Rev. D* **1996**, *53*, 5541–5578, [[gr-qc/9506063](#)].
79. Avdeev, N.; Dyadina, P.; Labazova, S. Test of hybrid metric-Palatini  $f(R)$ -gravity in binary pulsars. *J. Exp. Theor. Phys.* **2020**, *131*, 537–547, [[arXiv:gr-qc/2009.11156](#)].
80. Will, C.M. The Confrontation between General Relativity and Experiment. *Living Rev. Rel.* **2014**, *17*, 4, [[arXiv:gr-qc/1403.7377](#)].
81. Bergmann, P.G. Comments on the scalar tensor theory. *Int. J. Theor. Phys.* **1968**, *1*, 25–36.
82. Chiba, T.  $1/R$  gravity and scalar - tensor gravity. *Phys. Lett. B* **2003**, *575*, 1–3, [[astro-ph/0307338](#)].
83. Olmo, G.J. The Gravity Lagrangian according to solar system experiments. *Phys. Rev. Lett.* **2005**, *95*, 261102, [[gr-qc/0505101](#)].
84. Olmo, G.J. Limit to general relativity in  $f(R)$  theories of gravity. *Phys. Rev. D* **2007**, *75*, 023511, [[gr-qc/0612047](#)].
85. Koivisto, T.; Kurki-Suonio, H. Cosmological perturbations in the palatini formulation of modified gravity. *Class. Quant. Grav.* **2006**, *23*, 2355–2369, [[astro-ph/0509422](#)].
86. Koivisto, T. The matter power spectrum in  $f(r)$  gravity. *Phys. Rev. D* **2006**, *73*, 083517, [[astro-ph/0602031](#)].
87. Harko, T.; Koivisto, T.S.; Lobo, F.S.N.; Olmo, G.J. Metric-Palatini gravity unifying local constraints and late-time cosmic acceleration. *Phys. Rev. D* **2012**, *85*, 084016, [[arXiv:gr-qc/1110.1049](#)].
88. Capozziello, S.; Harko, T.; Koivisto, T.S.; Lobo, F.S.N.; Olmo, G.J. Hybrid metric-Palatini gravity. *Universe* **2015**, *1*, 199–238, [[arXiv:gr-qc/1508.04641](#)].
89. Nutku, Y. The Post-Newtonian Equations of Hydrodynamics in the Brans-Dicke Theory. *Astrophysical Journal* **1969**, *155*, 999.
90. Calmet, X.; Croon, D.; Fritz, C. Non-locality in Quantum Field Theory due to General Relativity. *Eur. Phys. J. C* **2015**, *75*, 605, [[arXiv:hep-th/1505.04517](#)].
91. Schwinger, J.S. Brownian motion of a quantum oscillator. *J. Math. Phys.* **1961**, *2*, 407–432.
92. Keldysh, L.V. Diagram technique for nonequilibrium processes. *Zh. Eksp. Teor. Fiz.* **1964**, *47*, 1515–1527.

93. Aad, G.; others. Search for contact interactions and large extra dimensions in the dilepton channel using proton-proton collisions at  $\sqrt{s} = 8$  TeV with the ATLAS detector. *Eur. Phys. J. C* **2014**, *74*, 3134, [[arXiv:hep-ex/1407.2410](https://arxiv.org/abs/hep-ex/1407.2410)].

© 2022 by the authors. Submitted to *Universe* for possible open access publication under the terms and conditions of the Creative Commons Attribution license (<http://creativecommons.org/licenses/by/4.0/>)